JACS
JOURNAL OF THE AMERICAN CHEMICAL SOCIETY
Communication
pubs.acs.org/JACS

Full-Range Intracellular pH Sensing by an Aggregation-Induced Emission-Active Two-Channel Ratiometric Fluorogen

Sijie Chen,[†] Yuning Hong,[†] Yang Liu,[†] Jianzhao Liu,[†] Chris W. T. Leung,[†] Min Li,[†] Ryan T. K. Kwok,[†] Engui Zhao,[†] Jacky W. Y. Lam,[†] Yong Yu,[†] and Ben Zhong Tang*[,†,‡,§]

[†]Division of Biomedical Engineering, Department of Chemistry, Institute for Advanced Study, and Institute of Molecular Functional Materials, The Hong Kong University of Science & Technology (HKUST), Clear Water Bay, Kowloon, Hong Kong, China

[‡]Guangdong Innovative Research Team, SCUT−HKUST Joint Research Laboratory, State Key Laboratory of Luminescent Materials and Devices, South China University of Technology (SCUT), Guangzhou 510640, China

[§]HKUST Shenzhen Research Institute, Nanshan, Shenzhen 518057, China

Supporting Information

ABSTRACT: Intracellular pH (pH_i) is an important parameter associated with cellular behaviors and pathological conditions. Sensing pH_i and monitoring its changes in live cells are essential but challenging due to the lack of effective probes. We herein report a pH-sensitive fluorogen for pH_i sensing and tracking. The dye is a tetraphenylethene−cyanine adduct (TPE-Cy). It is biocompatible and cell-permeable. Upon diffusing into cells, it responds sensitively to pH_i in the entire physiological range, visualizing the acidic and basic compartments with intense red and blue emissions, respectively. The ratiometric signal of the red and blue channels can thus serve as an indicator for local proton concentration. The utility of TPE-Cy in pH_i imaging and monitoring is demonstrated with the use of confocal microscopy, ratiometric analysis, and flow cytometry.

Cells, the smallest units of life, are highly organized.[1] The cellular compartments require proper conditions to perform their normal functions. Intracellular pH (pH_i) is an essential factor that regulates many cellular behaviors, including proliferation and apoptosis as well as enzyme activity and protein degradation.[2] In a typical mammalian cell, the pH_i can vary from 4.7 in lysosome to 8.0 in mitochondria. Disruptive variation in the pH_i may lead to dysfunction of the organelles. Abnormal pH_i is a hallmark of many common diseases such as cancer, stroke, and Alzheimer's disease. Sensing and monitoring pH changes inside living cells are thus of great importance for studying cellular metabolisms and gaining insights into physiological and pathological processes.[2,3]

A number of methods, such as H^+-permeable microelectrodes, ^{31}P NMR spectroscopy, and optical microscopy, have been used to measure pH_i.[3] Fluorescence-based techniques are the most powerful tools for assessing intact and subcellular pH, owing to their high sensitivity and unrivaled spatiotemporal resolution. Supporting techniques such as fluorescence microscopy and flow cytometry for high-resolution and high-throughput analysis are technically mature and readily accessible.[4] The development of pH-sensitive fluorescent indicators is thus the threshold of using fluorescence for pH_i sensing and mapping.

Scheme 1. Working Principle: Fluorescent Response of TPE-Cy to pH Change

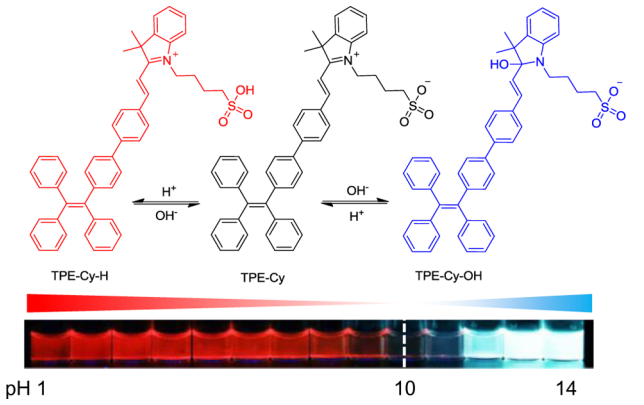

Much research effort has been devoted to the development of new pH sensors, including organic dyes,[5] nanoscale particles,[6] and fluorescent proteins.[7] Most of the sensors, however, are single-wavelength indicators whose fluorescence intensities vary with the changes in pH. The difference in the fluorescence signals is dependent on dye concentration and optical path length.[8] Their sensing spans are too narrow to cover the whole pH_i range.[3,5−7,9,10] To achieve full-range pH_i sensing, different pH-sensitive dyes have been doped into nanoparticle matrixes.[6] Whereas the sensing range is widened and the response pattern becomes ratiometric, the fabrication of multicomponent nanoparticles is a nontrivial task that requires precise control over the ratios of the dyes and their distributions in the matrixes. Meanwhile, the nanoparticles usually enter cells via endocytosis processes. Their intracellular distributions and sensing regions are restricted to the endocytic compartments instead of the entire cytoplasm. The best approach is thus to develop a cell-permeable ratiometric sensor with a broad pH-response window.

Recently, our group has developed a pH-responsive fluorogen consisting of tetraphenylethene (TPE) and cyanine (Cy) units.[11] It displays a large Stokes shift (>185 nm) and exhibits aggregation-induced emission (AIE) feature,[12] overcoming the

Received: January 11, 2013
Published: March 18, 2013

   dx.doi.org/10.1021/ja400337p | J. Am. Chem. Soc. 2013, 135, 4926−4929

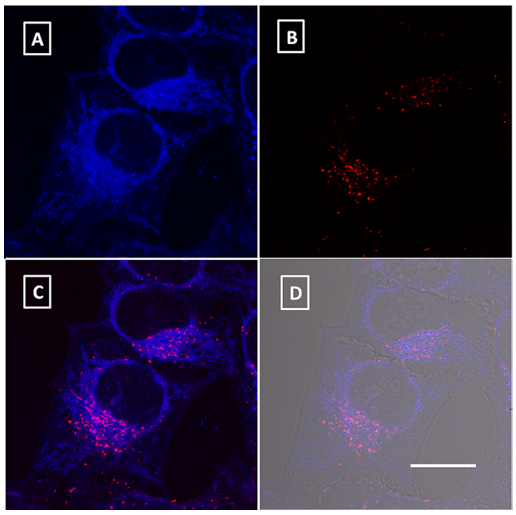

Figure 1. Confocal images of HeLa cells incubated with TPE-Cy for 2 h under excitation of (A) 405 and (B) 488 nm. (C) Image merged from those in panels A and B. (D) Image merged from that in panel C and the bright-field image. Scale bar, 20 μm. [TPE-Cy] = 10^{-5} M.

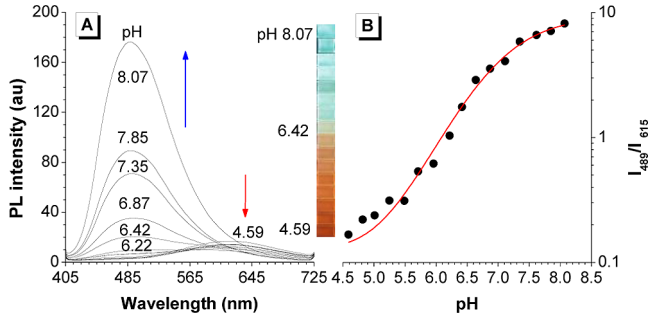

Figure 2. (A) Emission spectra and (inset) fluorescence photographs of TPE-Cy in the buffer solutions with different pH values in the presence of 1,2-dioleoyl-glycero-3-phosphocholine (DOPC). [TPE-Cy] = 10^{-5} M; [DOPC] = 0.1 mg/mL. (B) Plot of I_{489}/I_{615} versus pH. I_{489} and I_{615} denote the emission intensities of the solution at 489 and 615 nm, respectively. Excitation wavelength, 380 nm.

limitations imposed by the concentration quenching problem encountered by most conventional dyes. The AIE attribute of TPE-Cy and its reactivity with OH^-/H^+ enable it to sense pH in a broad range—the broadest to date.[11] TPE-Cy shows strong-to-medium red emissions at pH 5−7, weak-to-nil red emissions at pH 7−10, and nil-to-strong blue emissions at pH 10−14 (Scheme 1). A linear relationship of its fluorescence intensity with pH is established in the physiological range (pH 5.0−7.4), making it promising as a fluorescent indicator for pH_i sensing. In this work, we explore the utility of TPE-Cy for sensing subcellular pH and monitoring pH_i change in living cells. The transition point of its red-to-blue emission is found to shift from extracellular pH 10 to intracellular pH 6.5, facilitating the full-range pH_i sensing in a ratiometric manner.

For a probe to be used in live cells, biocompatibility is always the first property to examine.[13] The cytotoxicity of the TPE-Cy fluorogen was evaluated using a 3-(4,5-dimethyl-2-thiazolyl)-2,5-diphenyltetrazolium bromide (MTT) assay. The results show that the cell viability is not obviously affected even when a TPE-Cy concentration as high as 12.5 μM is used in the culture medium (Figure S1).

The excellent biocompatibility of the fluorogen prompted us to further investigate its performance in cell imaging. Our previous observations revealed that, in pure buffer solutions, the blue emission was predominant only at pH >10.[11] We thus expected that, inside a cell, the red emission should be observed, with its signal intensified with increasing acidity. TPE-Cy fluorogen is cell permeable. After entering a live cell, its molecules distribute in the cytoplasm, accumulate in certain organelles, and become fluorescent due to its AIE property (Figure 1). To our surprise, however, the majority of the cytoplasmic region stained by TPE-Cy emits strong blue light upon excitation at 405 nm (Figure 1A). With excitation at a longer wavelength of 488 nm, red signals can be detected but in a pattern different from that of the blue ones (Figure 1B,C).

We speculated that the pK_a of the TPE-Cy fluorogen may have been changed by its interaction with some biomolecules in the cells.[14] Close inspection of the subcellular distribution of the dyes reveals that the stained parts include tubular mitochondria and some other membrane-bound organelles but exclude nucleus, as verified by the data from co-localization with Rhodamine 123, a commercial dye specific to mitochondria (Figure S2). Since the major component of the membrane is phospholipids, phosphatidylcholine—the most abundant phospholipid—is chosen to test our hypothesis. As shown in Figure 2A, in the presence of 1,2-dioleoyl-glycero-3-phosphocholine (DOPC), a model phosphatidylcholine, TPE-Cy gives a strong blue emission peaked at 489 nm at a neutral pH. Alkalization to 8.07 results in an enhancement in this blue peak. On the other hand, acidification of the medium causes a decrease in the blue emission at 489 nm and induces the emergence and enhancement of the red emission at 615 nm. The two emission peaks are well separated and can be readily distinguished by fluorescence microscopy. The intensity ratio of the two emission peaks (I_{489}/I_{615}) increases nearly 50 times when the pH is changed from 4.59 to 8.07 (Figure 2B). The transition point of the red-to-blue emission is at pH ~6.42, much lower than that in the absence of DOPC (pH ~10, see Scheme 1).[11]

With the understanding of emission of TPE-Cy in the lipid-containing environment, we can conclude that, in the live cell images of Figure 1, the red signals come from the acidic organelles, while the regions with strong blue emission are more alkalescent. To further support this conclusion, a co-staining experiment of TPE-Cy with LysoTracker Green, a commercially available lysosome imaging agent, was conducted. Confocal cell images confirm that the red and green signals respectively from TPE-Cy (Figure 3A) and LysoTracker Green (Figure 3B) inside the cells, shown as punctate fluorescent spots, are localized in almost the same area (Figure 3C). Evidently, the red signals of TPE-Cy are indeed localized in lysosomes, the most acidic organelles.

Since the ratio of the blue-to-red signals from TPE-Cy corresponds to the local pH, mapping of pHi in the cytoplasmic region can be achieved through analysis of this ratio (Figure 3D). The area with pseudo red color, corresponding to a low blue-to-red ratio, suggests an acidic environment, while the pseudo blue color, with a higher ratio, indicates a higher pH. In the ratiometric image, the red color close to the perinuclear regions can be co-localized with the signal from LysoTracker Green in the green channel (Figure 3B), indicative of an acidic environment. Co-localization of TPE-Cy with Rhodamine 123 suggests that the blue-color area surrounding the red-color region in Figure 3D is mainly the mitochondria with higher local pH (Figure S4). The pH of other parts in cytoplasm with green and yellow colors should be in between.

dx.doi.org/10.1021/ja400337p | J. Am. Chem. Soc. 2013, 135, 4926−4929

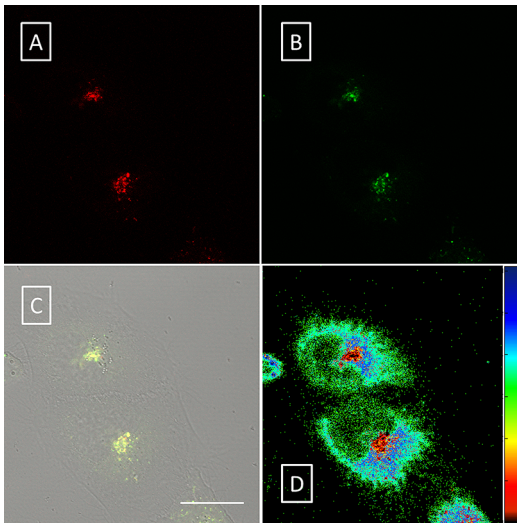

Figure 3. Confocal images of HeLa cells stained with (A) TPE-Cy and (B) LysoTracker Green. Excitation wavelength, 488 nm. Emission ranges: (A) 565−671 and (B) 513−542 nm. (C) Image merged from those of bright-field and panels A and B. (D) Ratiometric fluorescent image of the HeLa cells stained by TPE-Cy, shown in pseudo colors with red and blue indicating low and high blue-to-red emission ratios, respectively. The blue signal from TPE-Cy in this figure is given in Figure S3. Scale bar, 20 μm.

We then examined the response of this ratio to pH_i change. After staining and washing, the cells are incubated in the medium buffered with HEPES, which is used to keep a constant pH (7.4) of the solution. The ratiometric image shown in Figure 4D partitions the cells in the field of view according to their local pH. The portion of the acidic area accounts for less than 15% (log ratio $\leq$3) in the cells, as can be seen from the statistical analysis data for each pixel in the image (Figure 4A). To adjust the pH_i, acetic acid, a cell-permeable weak acid,[3,15] is employed to treat the living cells stained by TPE-Cy. Upon treatment with acetic acid, the acidic area with pseudo red color expands greatly (Figure 4E). The acidic compartments now occupy more than 20% area in the cell (Figure 4B), clearly demonstrating the acidification effect. When acetic acid is removed and replaced with DMEM (pH 8.5), regions with high blue-to-red ratio dominate the intracellular area (pseudo blue regions in Figure 4F), with the acidic regions shrunken. Consistent with the change in the pH distribution, the fractions of the areas with high blue-to-red ratios are increased (Figure 4C).

Confocal microscopy offers high spatial resolution but with limited data sampling. To test the feasibility of using TPE-Cy for high-throughput analysis, we employed flow cytometry for live cell pH_i sensing. The cells stained with TPE-Cy give strong red and blue signals, which can be easily differentiated from the unstained cells (Figure S6A,B). In line with the results from the confocal images, after addition of acetic acid, the red emission signals are predominantly from TPE-Cy-stained cells (Figure 5A). The ratio of the blue-to-red signal is decreased (Figure 5B), indicative of a decrease in pH_i in these cells. In sharp contrast to acetic acid, ammonium chloride (NH_4Cl) is known to induce intracellular alkalization.[3,7b] Addition of 20 mM NH_4Cl triggers an increase in the blue signal and a decrease in the red signal of the stained cells (Figure 5A). The corresponding blue-to-red emission ratio is increased dramatically in comparison to those of the cells in PBS or treated with acetic acid, indicative of an alkalized environment inside the cells (Figure 5B).

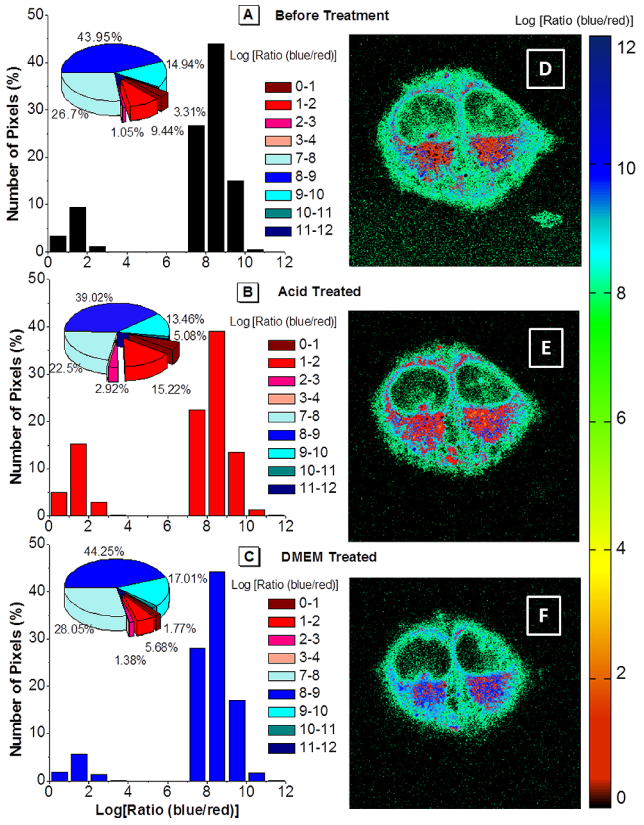

Figure 4. Distribution of blue-to-red emission ratio in confocal images of the HeLa cells (A) stained with TPE-Cy for 2 h, (B) treated with acetic acid for 10 min and (C) followed by treatment with Dulbecco's Modified Eagle Medium (DMEM) for 3 min. Inset in each panel is the pie chart for the same set of data. (D−F) Ratiometric fluorescent cell images in pseudo colors corresponding to the data shown in panels A−C. The bright-field and fluorescent images for this figure are shown in Figure S5.

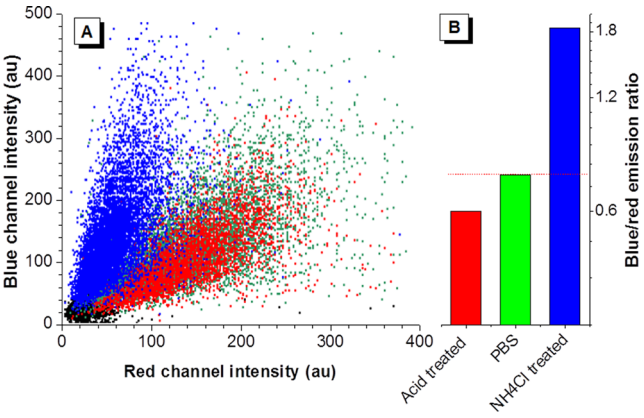

Figure 5. (A) Flow cytomerty analysis of HeLa cells stained with TPE-Cy. The cells in phosphate-buffered saline (PBS; green dots) were treated with acetic acid (red dots) or NH_4Cl (blue dots). The cells without staining are shown as control (black dots). Signals were collected from the blue channel (λ_{ex} = 375 nm, λ_{em} = 450 ± 20 nm) and red channel (λ_{ex} = 488 nm, λ_{em} = 610 ± 11.5 nm). (B) Comparison of the blue-to-red emission ratio in PBS with that treated with acetic acid or NH_4Cl.

The above results clearly demonstrate the utility of TPE-Cy for mapping and sensing of pH in live cells. To further evaluate its value for bioapplications, photostability and leakage assays were

dx.doi.org/10.1021/ja400337p | J. Am. Chem. Soc. 2013, 135, 4926−4929

performed. As shown in Figure S7, even after 50 scans with a total irradiation time of ~13 min, the signal loss of TPE-Cy is <13%, demonstrative of its superb photostability. Dye leakage from stained cells is an obstacle faced by many commercial pH_i sensors,[16] which hampers their use for tracking pH changes in live cells. As can be seen from Figure S8, after entering the cells, TPE-Cy can stay inside the live cells for ~1 h with <20% leakage, allowing its use for monitoring pH_i change over time.

It has become clear that the presence of lipid compartments such as DOPC facilitates the TPE-Cy fluorogen to shift its pK_a in physiological conditions, but how does the lipid alter the color transition point of the fluorogen? Taking into consideration the amphipathic character of phospholipids, we investigated whether the charges of the polar head and hydrophobic tails promote chemical reactions of TPE-Cy under physiological conditions. First, we measured the emission of TPE-Cy in the presence of lipids with different types of charged species between pH 5 and 7. The data show that only the positively charged lipids cause TPE-Cy to give a blue emission at pH 7 (Figure S9). To see whether a positive charge is the exclusive factor, the emission behaviors of TPE-Cy in the presence of various positively charged substances at different pHs were examined. In comparison to the photoluminescence spectrum in the presence of hexadecyltrimethylammonium—a cationic surfactant with a long fatty chain—tetramethylammonium chloride and NH_4Cl hardly shift the spectra to the blue region in the pH range of 5−7, revealing the involvement of the fatty alkyl chain (Figure S10). These experimental data suggest the following working mechanism: in the presence of phosphatidylcholine, the negatively charged sulfonate group of TPE-Cy is anchored by the positive head of the lipid, whereas the hydrophobic TPE core is immobilized by the fatty acid chains. These interactions may stabilize the basic form of TPE-Cy (i.e., TPE-Cy-OH shown in Scheme 1), thus shifting the equilibrium of the reaction toward the TPE-Cy-OH side and promoting the addition reaction to take place under the neutral condition.

In summary, we have developed a small organic fluorogen with AIE characteristics, TPE-Cy, for intracellular pH sensing in living cells. The TPE-Cy fluorogen is pH sensitive, and its emission color changes from red to blue with increasing pH. TPE-Cy is cell-permeable and enjoys excellent biocompatibility. Upon interacting with the lipid components of the cells, TPE-Cy shifts its color transition point of the red-to-blue emission from extracellular pH 10 to intracellular physiological pH range. The dynamic range of TPE-Cy for pH_i sensing thus covers the whole pH_i window from 4.7 to 8.0, which cannot be achieved by the majority of conventional pH_i indicators. Furthermore, pH_i sensing by TPE-Cy is in a ratiometric manner, in which the ratio of fluorescent intensity from two separate peaks is collected, circumventing interference from the uneven dye distribution as well as other technical artifacts. TPE-Cy has been successfully applied for pH_i imaging and monitoring with the use of confocal microscopy, ratiometric analysis, and flow cytometry, demonstrating its great potential for high-resolution and high-throughput analysis of intracellular environments which may find an array of biomedical applications in cancer diagnosis and drug screening.

■ ASSOCIATED CONTENT

Supporting Information

Experimental details and emission spectra of TPE-Cy in buffer solutions at different pHs in the presence of different lipids. This material is available free of charge via the Internet at http://pubs.acs.org.

■ AUTHOR INFORMATION

Corresponding Author

tangbenz@ust.hk

Notes

The authors declare no competing financial interest.

■ ACKNOWLEDGMENTS

We thank Teh Seng Khoon, Zhang Wei, and Zeng Yan for technical support on MATLAB programming. This work was partially supported by National Basic Research Program of China (973 Program; 2013CB834701), the Research Grants Council of Hong Kong (604711, 602212, HKUST2/CRF/10 and N_HKUST620/11), and the University Grants Committee of Hong Kong (AoE/P-03/08). B.Z.T. thanks Guangdong Innovative Research Team Program for support (201101C0105067115).

■ REFERENCES

(1) Albers, B.; Bray, D.; Hopkin, K.; Johnson, A.; Lewis, J.; Raff, M.; Roberts, K.; Walter, P. *Essential Cell Biology*, 3rd ed.; Garland Science: New York, 2009.

(2) Casey, J. R.; Grinstein, S.; Orlowski, J. *Nat. Rev. Mol. Cell Biol.* **2010**, *11*, 50.

(3) (a) Roos, A.; Boron, W. F. *Physiol. Rev.* **1981**, *61*, 296. (b) Srivastava, J.; Barber, D. L.; Jacobson, M. P. *Physiology* **2007**, *22*, 30.

(4) (a) *Optical Fluorescence Microscopy: From the Spectral to the Nano Dimension*; Diaspro, A., Ed.; Springer: New York, 2011. (b) *Flow Cytometry: Principles and Applications*; Macey, M. F., Ed.; Springer: Totowa, NJ, 2007.

(5) (a) Wang, R.; Yu, C.; Yu, F.; Chen, L. *Trends Anal. Chem.* **2010**, *29*, 1004. (b) Boens, N.; Qin, W.; Baruah, M.; De Borggraeve, W. M.; Filarowski, A.; Smisdom, N.; Ameloot, M.; Crovetto, L.; Talavera, E. M.; Alvarez-Pez, J. M. *Chem. Eur. J.* **2011**, *17*, 10924. (c) Basabe-Desmonts, L.; Reinhoudt, D. N.; Crego-Calama, M. *Chem. Soc. Rev.* **2007**, *36*, 993.

(6) (a) Shi, W.; Li, X.; Ma, H. *Angew. Chem., Int. Ed.* **2012**, *51*, 6432. (b) Zhou, K.; Liu, H.; Zhang, S.; Huang, X.; Wang, Y.; Huang, G.; Sumer, B. D.; Gao, J. *J. Am. Chem. Soc.* **2012**, *134*, 7803. (c) Marín, M. J.; Galindo, F.; Thomas, P.; Russell, D. A. *Angew. Chem., Int. Ed.* **2012**, *51*, 9657.

(7) (a) Llopis, J.; McCaffery, J. M.; Miyawaki, A.; Farquhar, M. G.; Tsien, R. Y. *Proc. Natl. Acad. Sci. U.S.A.* **1998**, *95*, 6803. (b) Tantama, M.; Hung, Y. P.; Yellen, G. *J. Am. Chem. Soc.* **2011**, *133*, 10034.

(8) *Epithelial Transport: a Guide to Methods and Experimental Analysis*; Wills, N. K., Reuss, L., Lewis, S. A., Eds.; Chapman & Hall: London, 1996.

(9) (a) Han, J.; Burgess, K. *Chem. Rev.* **2010**, *110*, 2709. (b) Venn, A. A.; Tambutté, E.; Lotto, S.; Zoccola, D.; Allemand, D.; Tambutté, S. *Proc. Natl. Acad. Sci. U.S.A.* **2009**, *106*, 16574.

(10) *The Molecular Probes Handbook*, 11th ed.; Jonhson, I., Spence, M. T. Z., Eds.; Invitrogen Corp.: Carlsbad, 2010; p 886.

(11) Chen, S.; Liu, J.; Liu, Y.; Su, H.; Hong, Y.; Jim, C. K. W.; Kwok, R. T. K.; Zhao, N.; Qin, W.; Lam, J. W. Y.; Wong, K. S.; Tang, B. Z. *Chem. Sci.* **2012**, *3*, 1804.

(12) (a) Hong, Y.; Lam, J. W. Y.; Tang, B. Z. *Chem. Commun.* **2009**, 4332. (b) Hong, Y.; Lam, J. W. Y.; Tang, B. Z. *Chem. Soc. Rev.* **2011**, *40*, 5361.

(13) Johnson, I. *Histochem. J.* **1998**, *30*, 123.

(14) Opitz, N.; Merten, E.; Acker, H. *Pflug. Arch. Eur. J. Phys.* **1994**, *427*, 332.

(15) Lyall, V.; Alam, R. I.; Phan, D. Q.; Ereso, G. L.; Phan, T.-H. T.; Malik, S. A.; Montrose, M. H.; Chu, S.; Heck, G. L.; Feldman, G. M.; DeSimone, J. A. *Am. J. Physiol. Cell Physiol.* **2001**, *281*, C1005.

(16) Salvi, A.; Quillan, J. M.; Sadee, W. *AAPS Pharm. Sci.* **2002**, *4*, 21.